

# Monte-Carlo simulation of cement neutron field distribution characteristics in PGNAA

YANG Jianbo<sup>1,2,\*</sup> YANG Yigang<sup>1</sup> LI Yuanjing<sup>1</sup> TUO Xianguo<sup>2,3</sup> LI Zhe<sup>2</sup>  
LIU Mingzhe<sup>2,3</sup> CHENG Yi<sup>2</sup> MU Keliang<sup>4</sup> WANG Lei<sup>2</sup>

<sup>1</sup>Department of Engineering Physics, Tsinghua University, Beijing 100084, China

<sup>2</sup>Chengdu University of Technology, Chengdu 610059, China

<sup>3</sup>State Key Laboratory of Geohazard prevention & Geoenvironment Protection, Chengdu 610059, China

<sup>4</sup>Nuclear Power Institute of China, Chengdu 610005, China

**Abstract** The distribution characteristics of the neutron field in cement was simulated using the MCNP code to comply with the requirements of an online Prompt Gamma Neutron Activation Analysis system. Simulation results showed that the neutron relative flux proportion reduced with increasing cement thickness. When the cement thickness remains unchanged, the reduced proportion of thermal neutrons increases to a small extent, but the epithermal, intermediate, and fast neutrons will decrease according to the geometric progression. H element in the cement mainly affects the reduction of fast neutrons and other single-substance elements, e.g., O, Ca, <sup>56</sup>Fe, Si, and Al. It also slows down the reduction of the fast neutrons via inelastic scattering. O contributes more than other elements in the reduction of fast neutrons. Changing the H content affects the thermal, epithermal, intermediate, and fast neutrons, while changing the Ca, Fe, and Si contents only influences the thermal, epithermal, and intermediate neutrons; hence, there is little effect on the reduction of fast neutrons.

**Key words** Monte Carlo simulation, MCNP, Prompt gamma neutron activation analysis, Neutron field distribution, Neutron flux rate

## 1 Introduction

A prompt gamma neutron activation analysis (PGNAA) system, which is a nondestructive, highly efficient, and multi-element nucleus analyzing technology, is widely used in resources such as cement, coal, and building materials, as well as chemical, mining, and metallurgy industry. Compared with the traditional chemical analysis and the sampling laboratory analysis, PGNAA is an important technology in modern industrial production<sup>[1–3]</sup>. In practice, the design of the PGNAA system must be optimized to maximize the yield of the prompt gamma rays. The neutrons and gamma rays arising from the neutron source are severely harmful to

the human body. Processing and optimizing the various parameters of the PGNAA system setup under the irradiation of a neutron source is dangerous and time consuming. Thus, as an alternative, a numerical simulation technology was developed and computational methods gradually replaced some experiments. Several scholars have studied PGNAA along with the Monte Carlo Method. For example, Oliveira<sup>[4]</sup> optimally designed a PGNAA instrument for analyzing cement raw materials, Naqvi<sup>[5,6]</sup> studied the performances of a PGNAA system using different neutron sources, and Zhang<sup>[7]</sup>, Yang<sup>[8,9]</sup> and other researchers<sup>[10–16]</sup> studied the application of the Monte Carlo Method in the design of an online neutron activation analysis system. However, these studies still

Supported by National Natural Science Foundation for Distinguished Young Scholar (41025015), NSFC(40974065, 11105132), Province Key Technology R&D Program(2011FZ0055), National High Technology Research and Development Program of China (2012AA063501), the Basic Research for Application of Sichuan Province (2012JY0109); China Postdoctoral Science Foundation(2012M520245)

\* Corresponding author. E-mail address: yjb@cdut.edu.cn

Received date: 2011-11-10

raise questions on what should be studied to improve the performance of PGNAA. For instance, the number and distribution characteristics of fast and thermal neutrons impose a direct influence on the yield of prompt  $\gamma$  where PGNAA is used to measure the cement element composition. Therefore, research needs to be conducted regarding the distribution characteristics of the neutron field in cement.

In this paper, the Monte Carlo method (MCNP code) is used to conduct a simulation analysis in the cement neutron field. Several results were obtained, such as the relations between the relative flux of neutrons and the cement sample thickness, as well as the effects of H, O, Ca,  $^{56}\text{Fe}$ , Si, and Al on the reduction of neutrons and the influence of their contents on the neutron field. The study on the distribution characteristics of the neutron field can provide a reference for the design of a PGNAA system.

## 2 Simulation Model

The experiment used a  $^{252}\text{Cf}$  spontaneous fission neutron source, with an emissivity of  $2.3 \times 10^{12} \text{ s}^{-1} \cdot \text{g}^{-1}$ , a half-life of 2.64, and an average neutron energy of 2.3 MeV. Yang method<sup>[17]</sup> was adopted to study the distribution characteristics of the coal neutron field. Fig.1 shows the cross section of the distribution model of the cement neutron field, with a cement sphere radius of 100 cm and a density of  $2.25 \text{ g/cm}^3$ . The neutron source  $^{252}\text{Cf}$  is located at the center of the cement sphere, which is divided into 21 parts at a radius interval of 5 cm. The cement sample consisted of  $\text{SiO}_2$ ,  $\text{Al}_2\text{O}_3$ ,  $\text{Fe}_2\text{O}_3$ ,  $\text{Fe}_3\text{O}_4$ ,  $\text{CaO}$ ,  $\text{CaCO}_3$ ,  $\text{MgO}$ ,  $\text{SO}_3$ ,

$\text{K}_2\text{O}$ ,  $\text{Na}_2\text{O}$ , and  $\text{H}_2\text{O}$ . Table 1 shows the mass percentages of all these elements.

## 3 Results and Discussion

In the MCNP simulation, the neutron source is the isotropic point source. A Maxwell fission spectrum model<sup>[18]</sup> is used with the following expression.

$$f(E) = Ce^{(0.5-E/a)}$$

where,  $E$  is the neutron energy,  $a$  (1.42 MeV) corresponds to a nuclear temperature at the neutron emission, and  $C$  is a coefficient.

The ENDF/B-VI Rel.1 cross-section database is applied. An Intel (R) Core (TM) 2CPU T7200 @ 2.00 GHz computer is used to perform the computation. The simulation particle number is  $2 \times 10^7$ . The F2 tally is chosen to record separately the relative counting rates (one neutron count per unit area) for the thermal ( $E < 0.4 \text{ eV}$ ), epithermal (0.4 to 100 eV), intermediate (100 to 200 keV), and fast neutrons ( $E > 200 \text{ keV}$ ). The computation time requires approximately 2 h for each data point, with an error of less than 1%.

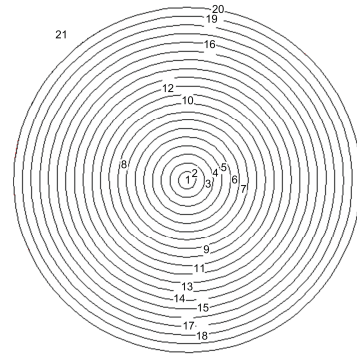


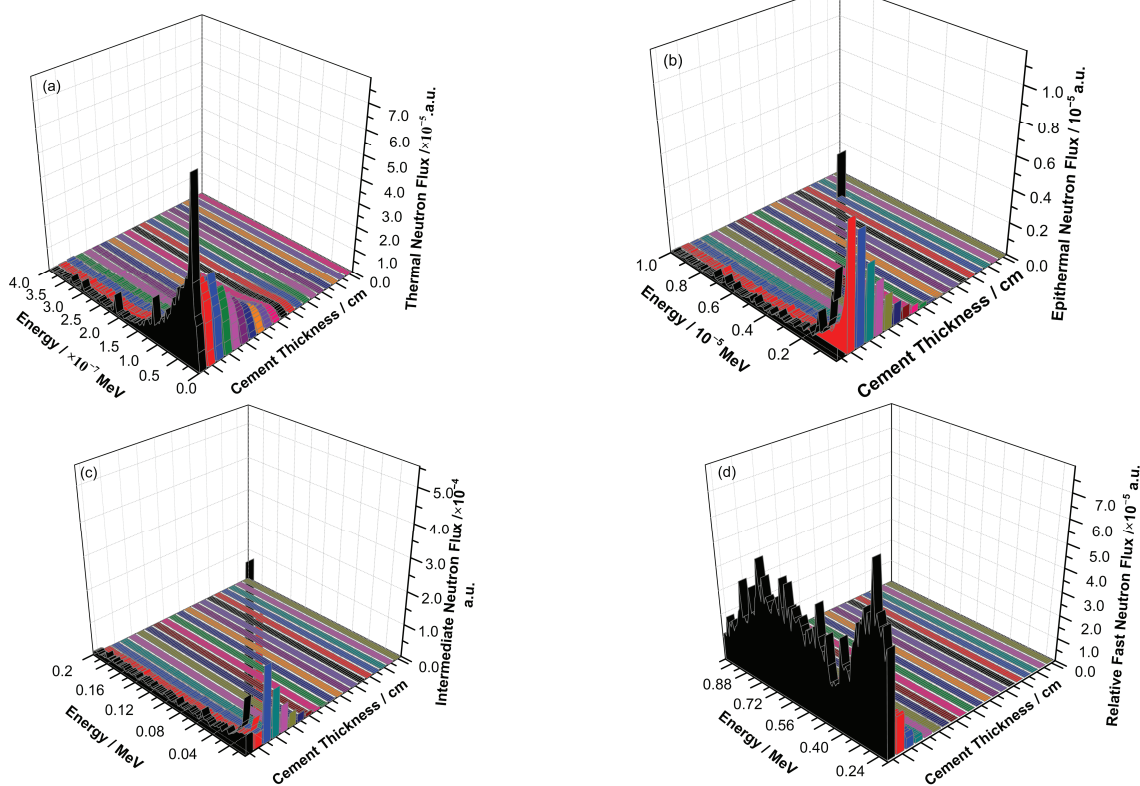
Fig.1 Sketch map of the simulation model section.

Table 1 Simulation of the elemental composition of the cement sample.

Element	Mass / %
H	8.476
O	60.409
Na	0.947
Mg	0.300
Al	2.483
Si	24.186
K	0.686
Ca	2.048
$^{54}\text{Fe}$	0.027
$^{56}\text{Fe}$	0.426
$^{57}\text{Fe}$	0.010
$^{58}\text{Fe}$	0.001

### 3.1 Simulation of Distribution of Cement Neutron Field

The relative counts of the thermal, epithermal, intermediate, and fast neutrons were recorded. These



**Fig.2** Relations between relative flux of neutrons and the cement thickness.

Figure 2a shows that the relative flux of thermal neutrons gradually decreases with the increase in cement thickness. The relative flux of thermal neutrons is centered in the area of cement with a thickness of less than 30 cm, and it is nearly zero in the area of cement with a thickness of more than 50 cm. The energy range of thermal neutrons mainly falls in the area below  $1.5 \times 10^{-7}$  MeV.

In Fig.2b, the relative flux of epithermal neutrons gradually decreases with the increase in cement thickness. The relative flux of epithermal neutrons reduces to a small proportion in the area of cement with a thickness of less than 40 cm. However, if the thickness was more than 40 cm, a big reduced proportion in the area of the cement could be found. The energy range of epithermal neutrons was mainly focused within the area below  $2 \times 10^{-5}$  MeV.

The relation between relative flux of intermediate neutrons and cement thickness is shown

values were used to identify the relations between the relative fluxes of neutrons and the cement thickness (Fig.2).

in Fig.2c. This figure is similar to Fig.2b, but the energy range of intermediate neutrons is mainly focused within the area below  $4 \times 10^{-2}$  MeV.

Figure 2d shows that cement thickness increases gradually with decreasing the relative flux of fast neutrons. The relative flux of fast neutrons is subjected to a small reduced proportion in the area of the cement with a thickness of less than 30 cm. In contrast, it is subjected to a big reduced proportion in the area of the cement with a thickness of more than 30 cm. When the cement thickness is small, every energy range of fast neutrons has a high relative flux.

The reduced proportions of relative flux of the thermal, epithermal, intermediate, and fast neutrons gradually rise with the increasing in cement thickness. The relative fluxes of fast and intermediate neutrons are subjected to the highest reduced proportion in the area of cement with a thickness of more than 30 cm according to the geometric progression. When the

cement thickness remains unchanged, the reduced proportions of epithermal, intermediate, and fast neutrons also decrease. The reduced proportion of epithermal neutrons is minimal while that of fast neutrons is maximal. The reduced proportion of thermal neutrons remains stable with the increase in cement thickness (Fig.3).

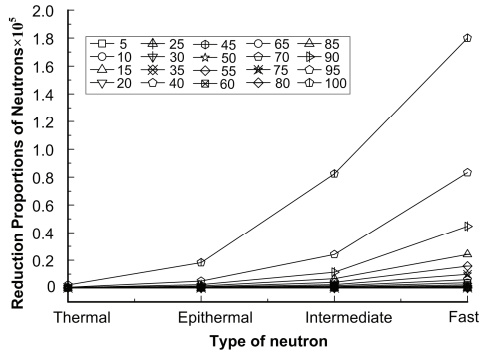


**Fig.3** Relations between the reduction proportions of neutrons and the type of neutron.

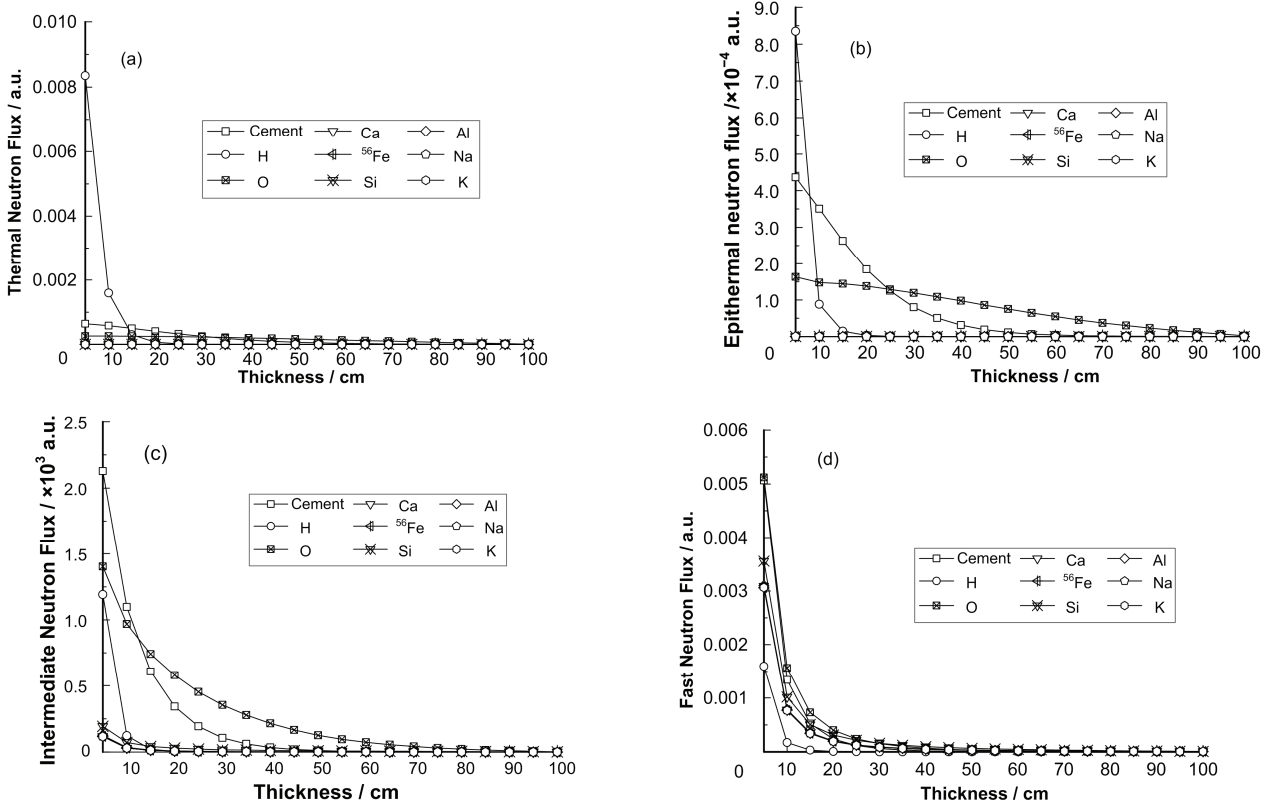


**Fig.4** Relations between the relative flux of neutrons and the thickness of cement and all single-substance elements.

Figures 4(a) and 4(b) show that the relative fluxes of thermal and epithermal neutrons gradually decrease with the increase in cement and the thickness of its elements. Consequently, given its strong moderation to fast neutrons, the relative flux of

### 3.2 Simulation of Distribution of Neutron Field of All Single-substance Elements

To understand better the contributions made by all the elements of the cement in the neutron field, the cement elements in the sphere were replaced with single-substance elements, namely, H, O, Ca,  $^{56}\text{Fe}$ , Si, Al, Na, K, etc. The assumption is that their density is the cement density and the product of percentage content individually, that is, each single-substance element is generally equal to its equivalent in the cement. A simulation computation is made to ascertain the alteration of thermal, epithermal, and fast neutrons with the thickness of all single-substance elements, as shown in Fig.4.

thermal and epithermal neutrons produced by H is higher than the ones generated by other single-substance elements and the cement. Meanwhile, H is more capable of absorbing thermal neutrons than other single-substance elements and the cement. If the

thickness is less than 15 cm, its reduced proportion is greater than other single-substance elements and cement. If the thickness is more than 15 cm, its relative fluxes of thermal and epithermal neutrons are several times less than other single-substance elements and the cement. All single-substance elements, except H and O, contribute little to the relative fluxes of the thermal and epithermal neutrons.

Figures 4c and 4d show that the relative fluxes of intermediate and fast neutrons gradually decrease with the increase in cement and the thickness of its elements. O can reduce intermediate and fast neutrons to some degree by a proportion bigger than the ones of other single-substance elements. If the thickness is less than 15 cm, its reduced proportion of intermediate and fast neutrons is very big. However, if the thickness is more than 15 cm, its reduced proportion of intermediate and fast neutrons gradually decreases.

The analysis shows that, the H plays a critical role in the formation of a cement neutron field at only 8.476% cement. With a nuclear mass of 1, H makes fast neutrons lose their half energy when they collide, causing thermal and epithermal neutrons to have a higher relative flux compared to other single-substance elements. Although possessing such capability, other single-substance elements slow down the reduction of the fast neutrons mainly through inelastic scattering.

**Table 2** Mass percentage content of cement sample after adjusting of H, Ca,  $^{56}\text{Fe}$ , and Si.

Added Elements	2%	4%	6%	8%
H	10.476	12.476	14.476	16.476
Ca	4.048	6.048	8.048	10.048
$^{56}\text{Fe}$	2.426	4.426	6.426	8.426
Si	26.186	28.186	30.186	32.186
O	58.409	56.409	54.409	52.409

After 2%, 4%, 6%, and 8% of H, Ca,  $^{56}\text{Fe}$ , and Si, are added (O will decline by 2%, 4%, 6%, and 8%), a simulation method is used to work out the relations between the relative fluxes of neutrons with different H and Ca contents and cement thickness, as shown in Figs.(5) and (6).

After the H content in the sample cement increased, Figs.5(a), (b), and (c) show that the relative flux of thermal neutrons increased slightly when the thickness was less than 30 cm. The relative fluxes of epithermal and intermediate neutrons increased

When the neutron energy is less than a particular inelastic scattering value, reduction only happens through elastic scattering, which plays a secondary role<sup>[17]</sup>. All single-substance elements can also slow down the reduction of intermediate and fast neutrons to some degree. The highest content of O in the cement probably makes O account for the biggest reduced proportion of intermediate and fast neutrons.

### 3.3 Influences of Content Change of H, Ca, Fe, and Si on the Distribution of Cement Neutron Field

The question is whether the content change of H, Ca, Fe, and Si would influence the distribution of the cement neutron field if the main compositions of the cement sample consist of  $\text{CaCO}_3$ ,  $\text{CaO}$ ,  $\text{Fe}_2\text{O}_3$ ,  $\text{Fe}_3\text{O}_4$ ,  $\text{SiO}_2$ , and  $\text{H}_2\text{O}$ . Despite taking up most in the cement, changing the O content has little influence on thermal neutrons because of its small absorbing cross section. When added with 2% H, 4% Ca, 6%  $^{56}\text{Fe}$ , and 8% Si, O will impose no influence if it is used for corresponding adjustments (making the general mass 100%). Table 2 shows the content of analog cement samples after H, Ca,  $^{56}\text{Fe}$ , and Si are adjusted. We observe the influence of content change of H, Ca, Fe, and Si on the distribution of cement neutron field.

slightly, while the relative flux stayed the same as the original value when the thickness was within 20–30 cm. This finding indicates that the thermal neutrons, which was moderated by the added H, was absolutely absorbed when the thickness was bigger than 30 cm. From Fig.5d, the relative flux of fast neutrons reduced slightly with the increase in thickness. This result indicates that fast neutrons were moderated into ones with lower energy, and little influence was produced on the fast neutrons.

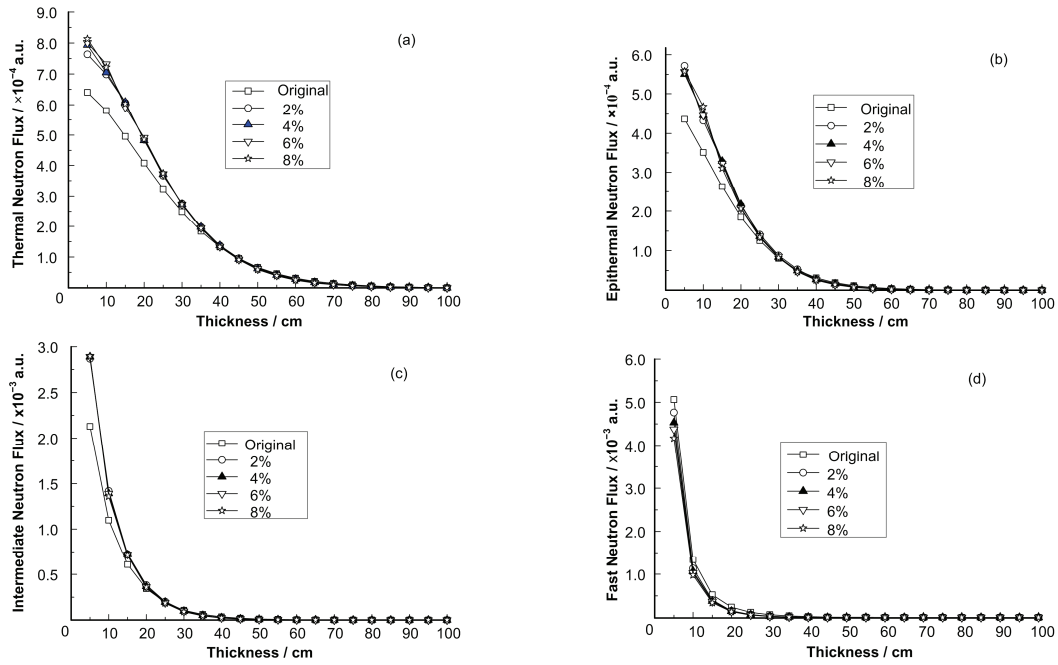


**Fig.5** Relations between the relative fluxes of neutrons with different H contents and the cement thickness.

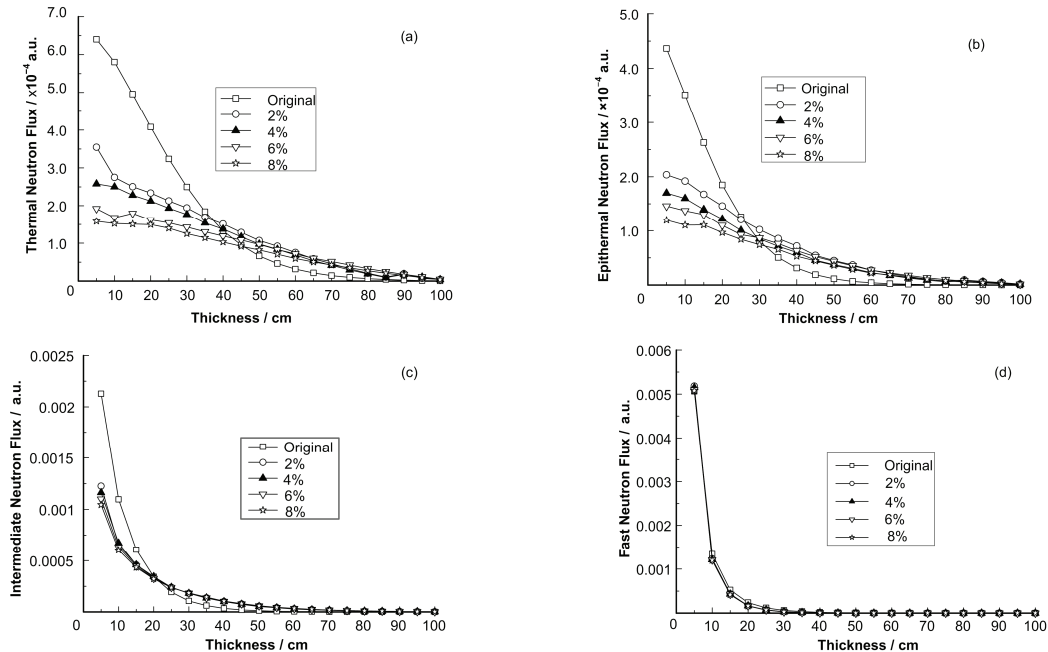


**Fig.6** Relations between the relative fluxes of neutrons with different Ca contents and the cement thickness.

Figures 6(a) and 6(b) show that Ca has a big thermal neutron absorption cross section and strong absorption capacity for thermal and epithermal neutrons. The thermal and epithermal neutron fields in the cement are influenced when their contents change. With the increase of Ca content, the relative fluxes of thermal and epithermal neutrons are reduced gradually. When the thickness is under 30 cm, the relative fluxes of thermal and epithermal neutrons are smaller than the original values. When the thickness is more than

30 cm, their relative fluxes are slightly bigger than the original values. When the thickness is less than 30 cm, the reduced proportions of relative fluxes of thermal and epithermal neutrons are bigger than when the thickness is more than 30 cm. All the thermal and epithermal neutrons will be absorbed gradually with a continuous increase in thickness.

In Figs.6 (c) and (d), the Ca influences the intermediate neutrons, but has poor damping capacity on fast neutrons. The results are the same with the

original values, and no change was made. Ca, Fe, and Si have large thermal neutron absorption cross sections, and the distribution of neutron fields in the cement are the same as the ones of Ca. Therefore, analyses regarding these elements were omitted.

The changes in H content influence the thermal, epithermal, intermediate, and fast neutrons. However, the changes in the contents of Ca, Fe, and Si only influences the thermal, epithermal, and intermediate neutrons, and the attenuation to fast neutrons is not obvious.

#### 4 Conclusions

In the neutron field of cement, the attenuation proportions of relative fluxes of thermal, epithermal, intermediate, and fast neutrons intensify with the increase in cement thickness. When the thickness is more than 30 cm, the fast and intermediate neutrons are attenuated in a geometric series. Under the same cement thickness, the proportions of relative fluxes of epithermal, intermediate, and fast neutrons are attenuated in a geometric series. The attenuation proportion of thermal neutrons rises with the increase of cement thickness, but the increased proportion is small and no obvious change is seen.

When the H in the cement collides with the fast neutrons, the energy of the fast neutrons will be averagely reduced to half; hence, the relative fluxes of the thermal and epithermal neutrons are higher than the ones of other elements. H plays a major role in the attenuation of fast neutrons while other elements attenuate the fast neutrons mainly through inelastic scattering. When the neutron energy is less than a certain value of inelastic scattering, the fast neutrons are attenuated through elastic scattering. Other elements play a secondary role in the attenuation of fast neutrons. The largest content of O in the cement accounts for its bigger attenuation proportion to the intermediate and fast neutrons than other elements.

The change of H content influences the thermal, epithermal, intermediate, and fast neutrons, but the changes of Ca, Fe, and Si contents hardly influence

these, and the attenuation to the fast neutrons is not noticeable.

#### References

- 1 Khang P D, Haia N X, Tana V H, *et al.* Nucl Instrum Meth Phys Res A, 2011, **634**: 47–51.
- 2 Naqvi A A, Garwan M A, Maslehuddin M, *et al.* Appl Radiat Isoto, 2010, **68**: 635–638.
- 3 Favalli A, Mehner H C, Ciriello V, *et al.* Appl Radiat Isoto, 2010, **68**: 901–904.
- 4 Oliveira C, Salgado J, Carvallio F G J Radioan Nucl Chem, 1997, **216**: 191–198.
- 5 Naqvi A A. Nucl Instrum Meth Phys Res A, 2003, **511**: 400–407.
- 6 Naqvi A A, Nagadi M M, Al-Amoudi O S B. Nucl Instrum Meth Phys Res A, 2005, **554**: 540–545.
- 7 Zhang F, Zhang G L. At Energy Sci Tech, 2006, **40**: 480–485.
- 8 Yang J B, Tuo X G, Mu K L, *et al.* At Energy Sci Tech, 2008, **42**: 329–332.
- 9 Yang J B, Tuo X G, LI Z, *et al.* Nucl Sci Tech, 2010, **21**: 221–226.
- 10 Tuo X G, Cheng B, Mu K L, *et al.* Nucl Sci Tech, 2008, **19**: 278–281.
- 11 Bai Y F, Wang D Z, MAUERHOFER Eric, *et al.* Nucl Sci Tech, 2010, **21**: 11–15.
- 12 Dong X Q, Luo W Y, Yue K, *et al.* Nucl Sci Tech, 2010, **21**: 16–19.
- 13 Xia M T, Liu Y Q, Sun X S, *et al.* Nucl Sci Tech, 2011, **22**: 144–150.
- 14 Liu Y, Xie T W, Liu Q, *et al.* Nucl Sci Tech, 2011, **22**: 165–173.
- 15 Sun H C, Ni B F, Zhang G Y, *et al.* Nucl Sci Tech, 2011, **22**: 287–292.
- 16 Feng P, Liu S Y, Wei B, *et al.* Nucl Sci Tech, 2011, **22**: 39–46.
- 17 Yang Y G. Research of on-line multi-element analysis by NIPGA technology (PhD Thesis), Beijing: Tsinghua University, 2001.
- 18 Briesmeister J F. MCNP-A general monte carlo N-particle transport Code (4C), Los Alamos, New Mexico: Los Alamos National Laboratory, 2000.